Journal of Neurosurgery Publishing Group Page Proof Policy

This page proof is a low-resolution PDF to reduce file size and download times. Figures in your article will appear as high-resolution images in the published versions of your article.

Your manuscript has been edited for content, consistency, and JNSPG style. Please be advised that all papers are run through a pre-editing program. Among other functions, the program converts British English to American English in all areas of the paper except the reference section.

- **PLEASE REVIEW THE PAGE PROOFS CAREFULLY!** This is the **only** opportunity to make minor changes to your article.

- Change only what is incorrect in the article. Limit your changes to **actual, necessary corrections** (not cosmetic, stylistic changes).

- It is the corresponding author's responsibility to ensure that all Disclosure information for each author is accurate and true.

- By returning the corrected page proofs (or approving the article as it now stands), the corresponding author attests to the fact that the final version of the paper has been approved by all authors.

- Substantive changes will require re-review of the article, leading to a delay in publication.

- Requested changes will be made at the discretion of the Editor.

Only **one** set of corrections will be accepted; please collaborate with your co-authors so that we do not receive conflicting corrections from several authors.

A PDF with high-resolution figures will be provided upon request.

Authors: Please review all authors' names, academic degrees, affiliations, and contributions, as well as the Disclosure, for spelling and accuracy.

Manuscript submission PDF

MS# 25-106, author proof

JNS

CLINICAL ARTICLE

Not for reprint

Morphological characteristics of healthy and aneurysmal internal carotid artery bifurcations

***Alexandra Lauric, PhD,[1,2] and Adel M. Malek, MD, PhD[1,2]**

[1]Department of Neurosurgery, Tufts Medical Center, Boston; and [2]Tufts University School of Medicine, Boston, Massachusetts

OBJECTIVE Internal carotid artery (ICA) bifurcation (ICAB) aneurysms carry high rupture risk, treatment challenges, and recurrence due to complex morphology and origination patterns. Given their relatively low incidence, research on ICAB morphology is limited. This study analyzed ICAB morphology in aneurysmal, contralateral, and healthy bifurcations, highlighting bilateral differences, anterior cerebral artery (ACA) dominance, and deviations from the vascular optimality principle (VOP).

METHODS A total of 194 angiographic volumes (40 aneurysmal, 28 contralateral, 126 healthy) were evaluated. ICAB morphology included parent/daughter vessel diameters and angle between the ICA and middle cerebral artery (MCA; Φ_{MCA}), angle between the ICA and ACA (Φ_{ACA}), total ICAB angle (Φ_{ICAB}; $\Phi_{MCA} + \Phi_{ACA}$). Aneurysm characteristics (size, neck, origination) and VOP parameters (radius ratio [RR] and junction exponent [*n*]) were evaluated. Bilateral analysis accounted for ACA dominance.

RESULTS Compared with controls, aneurysmal ICABs exhibited wider Φ_{MCA} (57.22° ± 12.22° vs 43.74° ± 9.41°, $p < 0.001$; area under the curve [AUC] = 0.83) and Φ_{ICAB} (160.27° ± 16.16° vs 143.66° ± 10.74°, $p < 0.001$; AUC = 0.79), but not Φ_{ACA}, in univariate, multivariate (AUC = 0.85), and bilateral analyses. Angle thresholds of 51.7° for Φ_{MCA} and 152.4° for Φ_{ICAB} were identified. Aneurysms originated predominantly off the apex (65%) and ACA (30%). Most occurred on ICABs with dominant (31%) and codominant (58%) A1 segments. Aneurysm neck, but not size, correlated with Φ_{MCA} and Φ_{ICAB}, but not Φ_{ACA}. In controls, Φ_{MCA} was larger and Φ_{ACA} smaller on the dominant A1 side, with no Φ_{ICAB} difference. There was no statistically significant difference in RR and *n* values regardless of aneurysm presence and dominance status.

CONCLUSIONS Aneurysmal ICABs have wider bifurcation angles that are more predominant on the MCA side compared with healthy controls. Only 10% of the aneurysms were found to occur on ICABs with the nondominant A1 segment. A1 dominance status influences bifurcation morphology not only in aneurysmal ICABs but also in healthy controls. These findings underline the importance of ICAB morphology for the likelihood of aneurysm presence, an association that can inform clinical decisions and may serve in predictive analytics.

https://thejns.org/doi/abs/10.3171/2025.8.JNS25106

KEYWORDS intracranial aneurysms; bifurcation morphology; internal carotid artery bifurcation aneurysms; vascular disorders

Cerebral bifurcations are arterial regions subject to increased hemodynamic stress, making them preferred sites for intracranial aneurysm formation.[1] Intracranial aneurysms, pathologic focal dilations of the cerebrovasculature, affect 3.6%–6% of the population. Although bifurcation aneurysms account for most cerebral aneurysms, internal carotid artery (ICA) bifurcation (ICAB) aneurysms occur at a low incidence, accounting for 2.4%–5% of all intracranial aneurysms.[2–4] Although relatively rare, these aneurysms are characterized by a high rupture rate of approximately 40%–50%[2,4] and are associated with multiple aneurysms[4] and younger age at diagnosis,[4,5] with a high prevalence in pediatric cases.[6] They also exhibit the lowest female predominance of all aneurysms (1:1.6).[5] Endovascular treatment of ICAB aneurysms can be challenging due to the bifurcation morphology and aneurysm origin that is often skewed off the apex toward either the middle cerebral artery (MCA) or anterior cerebral artery (ACA).[5] After treatment, ICAB aneurysms have a higher rate of recurrence (14%–22%) compared with aneurysms in other locations.[2]

While ICAB aneurysms have been studied in surgical

ABBREVIATIONS ACA = anterior cerebral artery; AUC = area under the curve; d_{ACA} = diameter of the ACA; d_{ICA} = diameter of the ICA; d_{MCA} = diameter of the MCA; ICA = internal carotid artery; ICAB = ICA bifurcation; MCA = middle cerebral artery; MPR = multiplanar reconstruction; *n* = junction exponent; r_{ACA} = radius of the ACA; r_{ICA} = radius of the ICA; r_{MCA} = radius of the MCA; ROC = receiver operating characteristic; RR = radius ratio; VOP = vascular optimality principle; Φ_{ACA} = angle between the ICA and ACA; Φ_{ICAB} = total ICAB angle; Φ_{MCA} = angle between the ICA and MCA.

SUBMITTED January 20, 2025. **ACCEPTED** August 6, 2025.

INCLUDE WHEN CITING Published online Month day, 2025; DOI: 10.3171/2025.8.JNS25106.

* A.L. and A.M.M. contributed equally to this work.

©AANS 2025, except where prohibited by US copyright law

Not for reprint

Low-resolution PDF

and endovascular contexts,[4,5,7] evaluations of aneurysmal and healthy ICAB morphology are limited and primarily based on small samples.[8,9] Most recently, Akdağ et al.[10] compared ICAB morphology between aneurysmal bifurcations and nonaneurysmal control bifurcations in patients with aneurysms in other locations. To the best of our knowledge, there are no larger studies comparing both healthy and aneurysmal ICAB morphology and comparing bilateral aneurysmal and nonaneurysmal contralateral ICAB morphology. In this study, we sought to examine ICAB morphology on healthy, aneurysmal, and nonaneurysmal contralateral bifurcations, including analysis of the vascular optimality principle (VOP)[8,9,11,12] and the effect of A1 dominance.

Methods

Patient Selection

High-resolution, 3D catheter angiographic volumetric datasets were analyzed for this study. ICAB aneurysm cases were included for analysis if the images were free of motion artifacts and provided sufficient quality for accurate processing and morphological analysis. If, during clinical care, 3D rotational angiography was performed on the nonaneurysm side, the bilateral data were also included in the analysis. Additionally, angiographic data from patients without cerebral aneurysms who underwent evaluation for unrelated medical conditions were considered if bilateral angiography of adequate quality was available. To ensure age matching between the aneurysm and control groups, patients younger than 20 years of age were excluded from the control group. All angiographic data within this set were obtained in an urgent fashion and prior to vasospasm onset.

This research was approved by the institutional review board ethics committee. Patient consent was waived due to the retrospective nature of the study not impacting patient clinical care.

Cerebral Angiography and Data Processing

Three-dimensional catheter-based cerebral angiograms were obtained using a calibrated biplane system. Volume reconstruction was performed with clinical software to create a 3D volumetric dataset (Fig. 1A). The reconstructed volumes were processed and analyzed using Amira visualization software (version 5.3.3, FEI), enabling segmentation of the aneurysm and adjacent vessels in 3D space.

Angiographic filling of the A1 segment was evaluated across all datasets, including healthy controls. The A1 segments were classified as dominant, nondominant, or codominant based on their size and angiographic appearance. Bilateral volumes were visualized and analyzed simultaneously using Amira 5.3 for enhanced comparative analysis (Figs. 1 and 2).

Angle Evaluation

A 3D vessel skeleton of the ICAB was generated in Amira using the auto-skeleton tool. Multiplanar reconstruction (MPR) was performed at the ICAB apex, guided by the local vessel centerline, to ensure that the plane was properly aligned with the center of the vessels (Fig. 1B). Measurements were performed manually, by a trained operator, using the centerline as guidance. The angle between the ICA and MCA was labeled as Φ_{MCA}, while the angle between the ICA and ACA was labeled as Φ_{ACA}. The total ICAB angle, Φ_{ICAB}, was defined as $\Phi_{ICAB} = \Phi_{MCA} + \Phi_{ACA}$. Angles were measured in the direction of flow (Fig. 1C), following the convention of Rossitti and Löfgren,[12] with measurements representing the deviation from the flow direction in the proximal segment.[8,12–15]

Caliber Evaluation

Three-dimensional gradient edge-detection filtering using the Sobel edge-detection filter was applied to avoid the operator bias involved in manual thresholding and level choice of the aneurysm surface, as described in the literature.[11,16] To guide the measurement process, an isosurface of the vasculature was also created using a threshold value and refined to align within the Sobel edges as previously described.[11,17]

Similar to the study by Baharoglu et al.[11] the measuring cutting planes were placed approximately 2 vessel diameters from the aneurysm neck or bifurcation point for each vessel in the bifurcation (Fig. 1B). If bifurcation morphology prevented measurements at a distance of 2 diameters, measurements were obtained sufficiently distally downstream. The vessels were sectioned in 3D space, and each cross-section was modeled as an ellipse to determine major and minor axes, enabling calculation of the mean vessel diameters. The mean ICA diameter was termed d_{ICA}, and the mean daughter branch diameters were termed, by convention, d_{MCA} for the MCA and d_{ACA} for the ACA (Fig. 1C–D). For aneurysmal bifurcations, the aneurysm neck origin was evaluated to determine if it emanated off of the apex of the bifurcation or off of one or the other of the daughter branches. Corresponding radii (r_{ICA}, r_{MCA}, r_{ACA}) were derived from the diameter measurement.

End-arterial bifurcations follow the VOP, obeying the principle of minimal work, based on vessel radii and bifurcation angles.[8] Although the ICAB is not a true end-bifurcation due to collateral flow via the anterior communicating complex, VOP parameters were assessed. The parent–to–daughter vessel radius ratio (RR) was calculated using the formula $r_{ICA}^3/(r_{MCA}^3 + r_{ACA}^3)$. Parent daughter branch ratios were calculated using the formula d_{ICA}/d_{MCA} and d_{ICA}/d_{ACA}. MATLAB software (MathWorks) was used to solve $r_{ICA}^n = r_{MCA}^n + r_{ACA}^n$ by bisection with inverse quadratic interpolation.[8,11] ACA dominance was determined based on flow characteristics and the relative caliber of the A1 segments.

Statistical Analysis

JMP statistical software (Version Pro 16, SAS Institute) was used to assess the performance of all parameters in distinguishing between the aneurysm and control ICAB datasets; $p < 0.05$ was considered statistically significant. Each variable was evaluated independently using the Student t-test. Bilateral analysis was conducted using matched-pair analysis. A receiver operating characteristic (ROC) curve was generated, and predictive accuracy was

Not for reprint

Low-resolution PDF

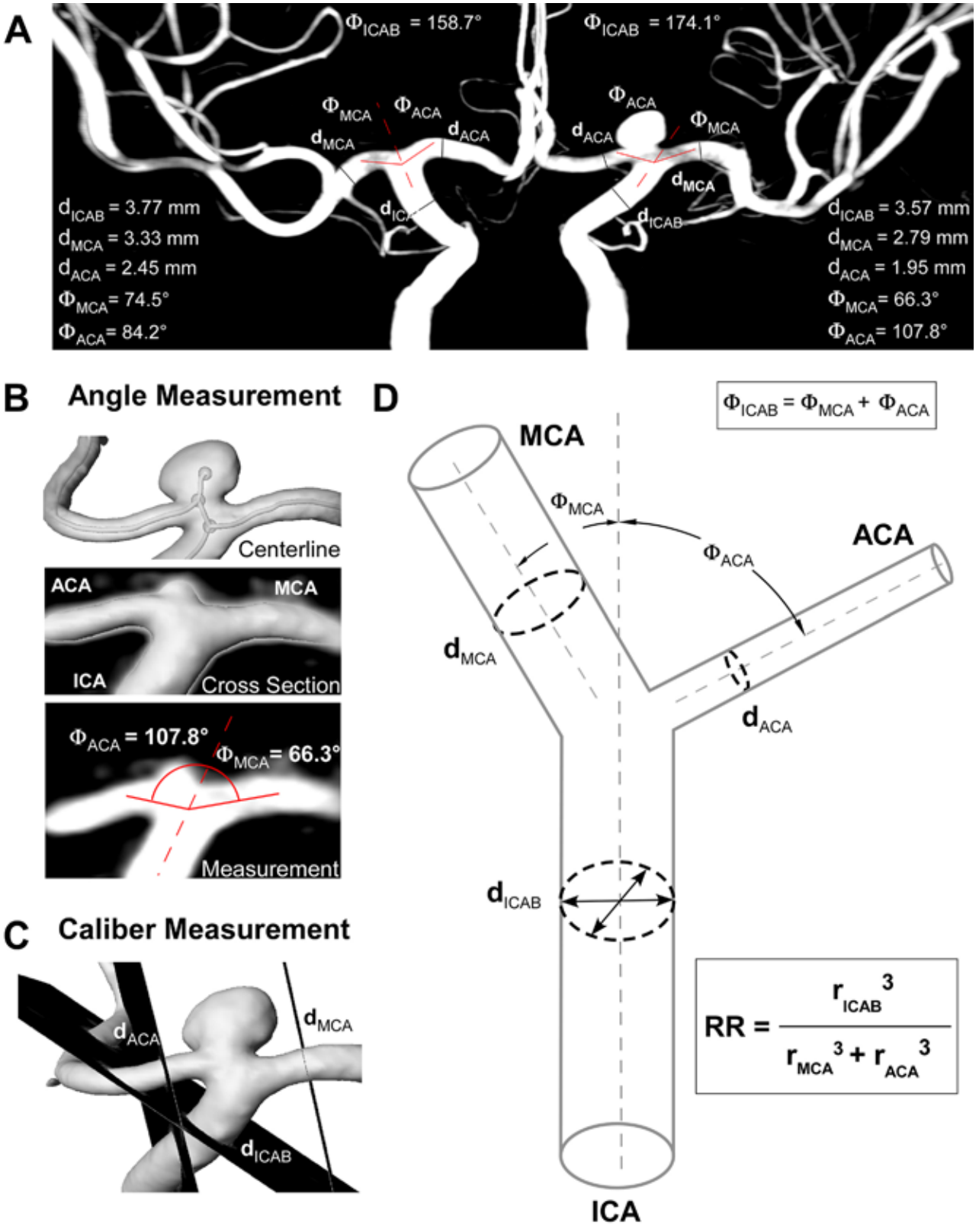


FIG. 1. A: Maximum intensity projection of an aneurysmal ICAB (*right*) visualized together with the corresponding control contralateral (*left*). **B:** Using the local vessel centerline as a guideline, MPR through the volume was evaluated at the ICAB apex for angle measurement in 2D cross-sections. **C:** Cross-sectional plane locations for vessel diameter evaluation. **D:** Schematic ICAB with measurement placement for angle and radii evaluation. Angles were measured in the direction of the flow with measurements representing the deviation from the direction of the flow in the proximal segment. Figure is available in color online only.

Not for reprint

Low-resolution PDF

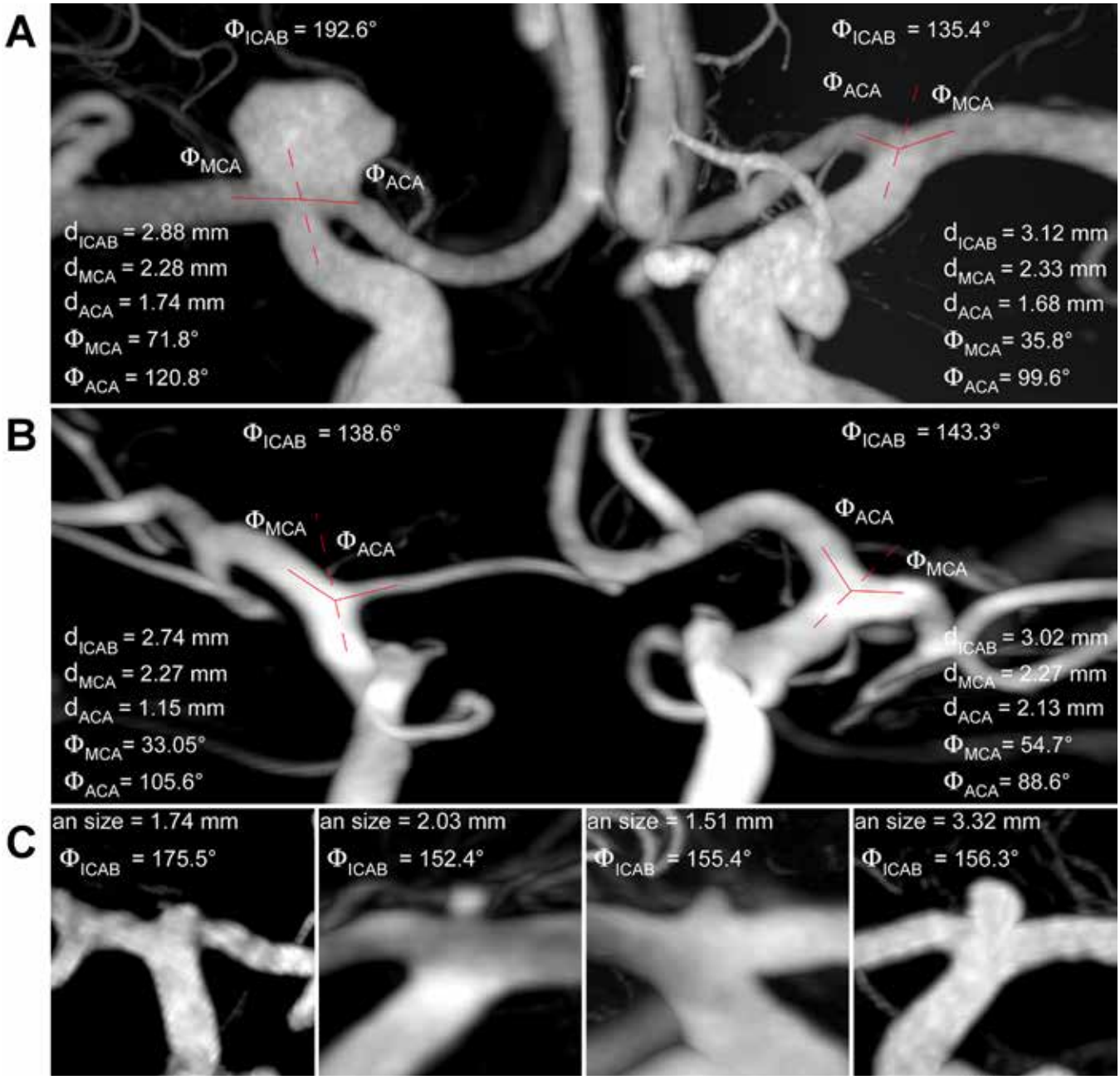


FIG. 2. A: Maximum intensity projection of an aneurysmal ICAB visualized together with the corresponding control contralateral. **B:** Maximum intensity projection of bilateral healthy ICABs with dominant (*right*) and nondominant (*left*) A1 segment labeling. **C:** ICABs harboring small (< 4 mm) aneurysms. An = aneurysm. Figure is available in color online only.

determined using the area under the curve (AUC) index. Optimal threshold values were established based on ROC statistics.

Results

Patient Demographics

A total of 194 3D rotational angiographic volumes were analyzed for this study. There were 40 aneurysmal ICAB samples (25 females; mean age 51.77 ± 12.17 years), 28 nonaneurysmal contralateral bifurcations (21 females; mean age 52.71 ± 10.49 years), and 126 non–aneurysm-bearing healthy samples (56 females; mean age 53.49 ± 14.17 years). There was no statistically significant difference in age between the three subgroups ($p = 0.77$). There were 5 ruptured aneurysms (12.5%, 2 females) in the dataset.

Aneurysmal ICAB Morphology

ICAB-harboring aneurysms had significantly wider Φ_{MCA}, Φ_{ACA}, and Φ_{ICAB} compared with nonaneurysmal

Not for reprint

Low-resolution PDF

TABLE 1. Univariate statistical analysis of ICAB morphological parameters in discriminating between aneurysmal and control samples

Feature	Mean ± SD			p Value		
	Aneurysmal, n = 40	Contralat, n = 28	Control, n = 126	Aneurysmal vs Contralat	Aneurysmal vs Control	Contralat vs Control
Φ_{MCA}, °	57.22 ± 12.22	41.79 ± 10.98	43.74 ± 9.41	**<0.001**	**<0.001**	0.65
Φ_{ACA}, °	103.05 ± 15.71	93.32 ± 12.00	99.91 ± 10.12	**0.003**	0.31	**0.03**
Φ_{ICAB}, °	160.27 ± 16.16	135.12 ± 12.69	143.66 ± 10.74	**<0.001**	**<0.001**	**0.004**
d_{MCA}, mm	2.54 ± 0.44	2.37 ± 0.51	2.55 ± 0.29	0.06	0.19	0.98
d_{ACA}, mm	1.96 ± 0.42	1.87 ± 0.49	1.99 ± 0.38	0.35	0.68	0.88
d_{ICA}, mm	3.17 ± 0.33	3.10 ± 0.54	3.21 ± 0.39	0.48	0.83	0.86
d_{ICA}/d_{MCA}	1.28 ± 0.22	1.36 ± 0.19	1.26 ± 0.13	0.09	0.45	0.75
d_{ICA}/d_{ACA}	1.68 ± 0.34	1.79 ± 0.69	1.66 ± 0.36	0.38	0.59	0.97
RR	1.47 ± 0.34	1.61 ± 0.65	1.36 ± 0.41	0.29	0.21	**0.02**
n	2.19 ± 0.14	1.96 ± 0.17	2.32 ± 0.81	0.32	0.44	0.06

Boldface type indicates statistical significance.

contralaterals (Table 1). In addition, aneurysmal ICABs had significantly wider Φ_{MCA} and Φ_{ICAB} compared with non–aneurysm-bearing healthy controls. There were no statistically significant differences between the three groups (aneurysmal, contralateral, and control) based on vessel caliber and vessel ratios. Univariate analysis repeated after the exclusion of ruptured aneurysms resulted in similar results. In addition, there was no statistically significant difference between ICAB-harboring ruptured and unruptured aneurysms for any of the morphological features studied here.

The Φ_{MCA} emerged as a strong discriminator between aneurysmal and control ICABs (57.22° ± 12.22° vs 43.74° ± 9.41°, $p < 0.001$; AUC = 0.83). A threshold of 51.7° for Φ_{MCA} was determined by ROC analysis (sensitivity 73%, specificity 85%). In contrast, Φ_{ACA} was not statistically significant in discriminating aneurysmal from healthy ICABs (103.05° ± 15.71° vs 99.91 ± 10.12°, $p = 0.31$; AUC = 0.59). Finally, Φ_{ICAB} was a strong discriminator between aneurysmal and healthy ICABs (160.27° ± 16.16° vs 143.66° ± 10.74°, $p < 0.001$; AUC = 0.79). A threshold of 152.4° for Φ_{ICAB} was determined by ROC analysis (sensitivity 70%, specificity 79%) (Fig. 3).

In multivariate analysis, Φ_{MCA} and Φ_{ICAB} combined resulted in an AUC of 0.85 (78% sensitivity, 78% specificity) in discriminating between aneurysmal and nonaneurysmal ICAB. Based on the Φ_{MCA} and Φ_{ICAB} identified thresholds, 5 of 40 (12.5%) aneurysmal ICABs would be misclassified as healthy bifurcations, and 11 of 126 (8.7%) healthy ICABs would be misclassified as aneurysmal.

Most aneurysms (n = 26, 65%) originated at the ICAB apex; 12 aneurysms originated off the A1 segment (30%), and only 2 aneurysms originated off the M1 segment (5%). In addition, most aneurysms occurred at the ICAB with dominant (9 aneurysms, 31%) and codominant (17 aneurysms, 58.6%) A1 segments. Only 3 aneurysms (10.3%) occurred on ICABs with a nondominant A1 segment.

Aneurysmal ICABs with nondominant A1 had significantly higher Φ_{ACA} (120.80° ± 17.94° vs 94.2° ± 13.42°, $p = 0.009$) and Φ_{ICAB} (170.46° ± 5.90° vs 149.35° ± 13.94°, $p = 0.05$) compared with the ICABs with dominant A1. As expected, nondominant ICABs had significantly smaller d_{ACA} and significantly larger d_{ICA}/d_{ACA} compared with dominant and codominant aneurysmal ICABs.

No correlation was found between age and Φ_{MCA}, Φ_{ACA}, and Φ_{ICAB} regardless of aneurysm presence status.

Effect of Aneurysm and Neck Size

The mean maximum aneurysm size of the dataset was 5.84 ± 3.19 mm. The dataset contained no giant aneurysms, defined as having a size larger than 25 mm. Four of the aneurysms were larger than 10 mm, and 9 aneurysms were smaller than 3 mm. Aneurysm size was not statistically significantly different between ruptured and unruptured aneurysms ($p = 0.86$). There was no statistically significant difference between smaller (< 3 mm) and larger aneurysms for any of the morphological features. However, smaller aneurysms tended to have smaller Φ_{MCA} (50.7° ± 10.98° vs 58.9° ± 12.56°, $p = 0.08$). Based on identified thresholds for Φ_{MCA} and Φ_{ICAB}, 4 of the 9 ICABs harboring small aneurysms would be misclassified as nonaneurysmal. No correlation was found between aneurysm size and Φ_{MCA}, Φ_{ACA}, or Φ_{ICAB}.

The mean aneurysm neck size of the dataset was 2.96 ± 1.11 mm. Neck size was not statistically different between ruptured and unruptured aneurysms ($p = 0.23$). A positive correlation was found between neck size and Φ_{MCA} ($p = 0.008$, $R^2 = 0.21$) and Φ_{ICAB} ($p < 0.001$, $R^2 = 0.37$), but not Φ_{ACA} ($p = 0.14$).

Healthy ICAB Morphology

As shown in Table 2, in healthy ICAB, Φ_{MCA} was significantly larger in dominant bifurcations (as defined by A1 segment classification) compared with nondominant bifurcations (mean 46.54° ± 8.69° vs 40.25° ± 8.90°, $p = 0.006$), but significantly smaller compared with aneurysmal samples (57.22° ± 12.22°, $p < 0.001$) (Table 1). In contrast, Φ_{ACA} was significantly smaller in dominant bifurcations compared with nondominant (94° ± 9.28° vs 104.32° ± 10.98°, $p < 0.001$) and also significantly smaller compared with aneurysmal samples (103.05° ± 15.71°, $p = 0.01$) whose values were similar to those observed in healthy nondominant bifurcations. Dominant and non-

Not for reprint

Low-resolution PDF

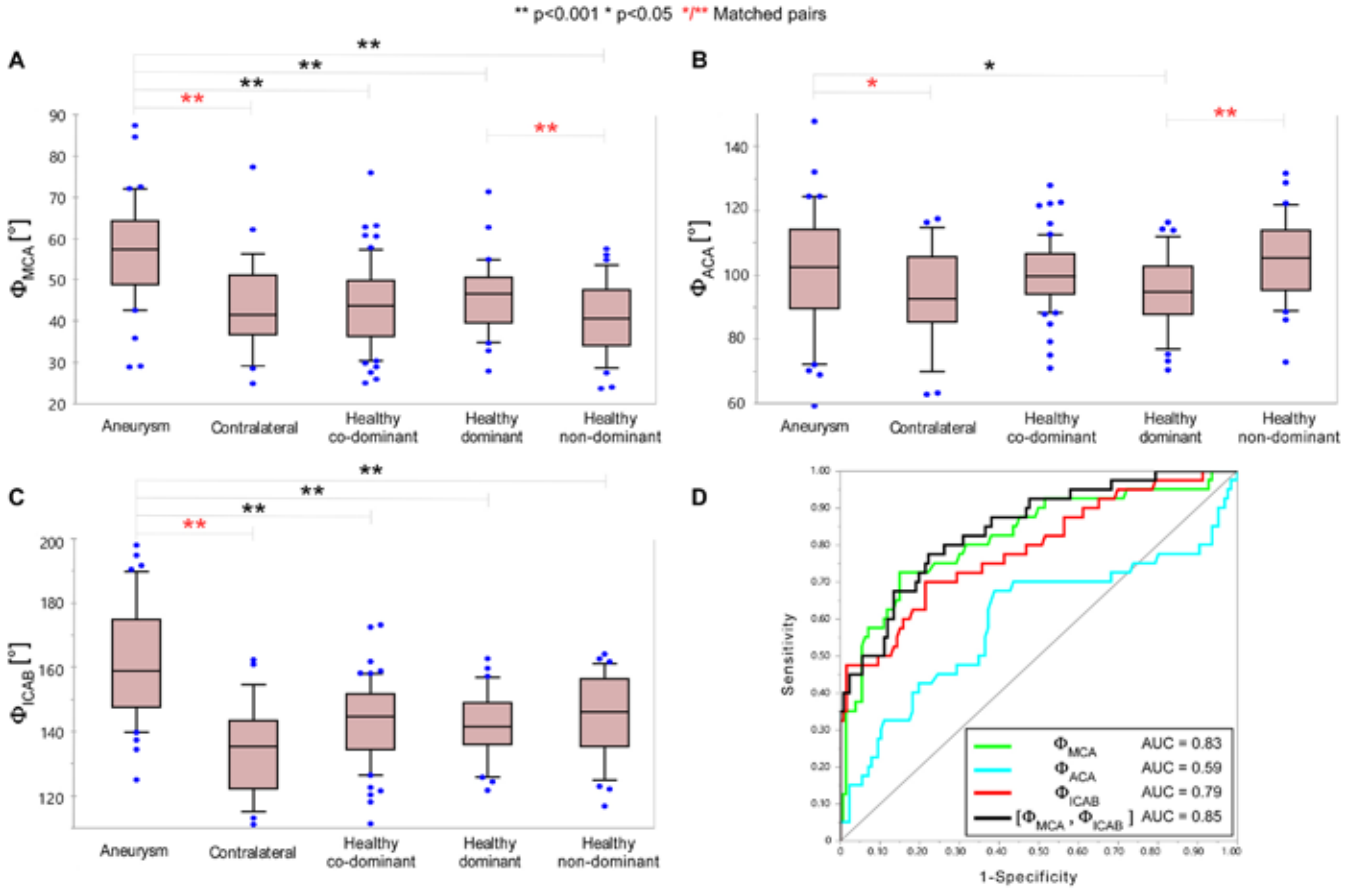


FIG. 3. A–C: Box plot visualizations of Φ_{MCA} (A), Φ_{ACA} (B), and Φ_{ICAB} (C). **D:** ROC curves of univariate and multivariate analyses for Φ_{MCA}, Φ_{ACA}, and Φ_{ICAB}. *Red asterisks* denote statistical significance in both univariate and matched pair analyses. Figure is available in color online only.

dominant healthy ICABs had similar Φ_{ICAB} (141.16° ± 9.35° vs 144.57° ± 12.21°, p = 0.19), which was significantly smaller compared with aneurysmal ICABs (160.27° ± 16.16°, p < 0.001).

As expected, compared with dominant healthy bifurcations, nondominant healthy bifurcations had significantly smaller ICA and ACA diameters compared with dominant sides but similar MCA diameters. The diameter ratio d_{ICA}/d_{MCA} (1.29 ± 0.13 vs 1.20 ± 0.13, p = 0.03) was significantly larger in dominant samples, whereas d_{ICA}/d_{ACA} was significantly smaller (1.49 ± 0.20 vs 1.98 ± 0.46, p < 0.001). Comprehensive analysis, stratified by aneurysm presence and A1 dominance status, is shown in Supplemental Table 1.

Matched-Pair Analysis

Bilateral imaging was available for 28 patients harboring unilateral ICAB aneurysms. Matched-pair analysis (Table 3), in which each patient acts as their own control, showed that Φ_{MCA}, Φ_{ACA}, and Φ_{ICAB} were significantly larger in aneurysmal bifurcations compared with the corresponding nonaneurysmal contralateral. However, there was no difference regarding radii, radii ratios, or VOP parameters.

In healthy patients, bilateral analysis confirmed the univariate analysis results and showed that Φ_{MCA} was significantly larger on the dominant side (ICAB with dominant A1 segment), while Φ_{ACA} was significantly smaller. There was no statistically significant difference in Φ_{ICAB} values between healthy ICABs with dominant versus nondominant A1 segments.

Vascular Optimality Principle

RR and *n* values were not significantly different regardless of aneurysm presence and dominance status. In the case of aneurysmal samples, the RR was 1.47 ± 0.34, whereas the RR for healthy bifurcation was 1.36 ± 0.41. In the case of aneurysmal samples, *n* was 2.19 ± 0.14, whereas for healthy bifurcation *n* was 2.32 ± 0.81 (Table 1).

Discussion

Although they have relatively low incidence, ICAB aneurysms have unique characteristics that impact clinical care and management options. These aneurysms have a high risk of rupture,[2] present treatment challenges, and have a high risk of recurrence due to ICAB distinct morphology.[2] ICAB aneurysms are diagnosed at younger ages compared with aneurysms in other locations,[5] and are predominant in pediatric cases.[6] Although female sex is an independent risk for aneurysm formation,[18] ICAB an-

Not for reprint

Low-resolution PDF

TABLE 2. Univariate statistical analysis of ICAB morphological parameters

Feature	Mean ± SD			p Value		
	HD, n = 33	HC, n = 60	HN, n = 33	HC vs HD	HN vs HD	HN vs HC
Φ_{MCA}, °	46.54 ± 8.69	44.15 ± 9.63	40.25 ± 8.90	0.23	**0.006**	0.05
Φ_{ACA}, °	94 ± 9.28	100.43 ± 8.72	104.32 ± 10.98	**0.005**	**<0.001**	0.06
Φ_{ICAB}, °	141.16 ± 9.35	144.59 ± 1.41	144.57 ± 12.21	0.14	0.19	0.99
d_{MCA}, mm	2.61 ± 0.27	2.49 ± 0.28	2.60 ± 0.31	0.14	0.19	0.98
d_{ACA}, mm	2.27 ± 0.30	2.04 ± 0.32	1.64 ± 0.37	**0.005**	**<0.001**	**<0.001**
d_{ICA}, mm	3.35 ± 0.42	3.18 ± 0.36	3.11 ± 0.41	0.11	**0.04**	0.71
d_{ICA}/d_{MCA}	1.29 ± 0.13	1.28 ± 0.13	1.20 ± 0.13	0.98	**0.03**	**0.02**
d_{ICA}/d_{ACA}	1.49 ± 0.20	1.58 ± 0.24	1.98 ± 0.46	0.34	**<0.001**	**<0.001**
RR	1.29 ± 0.35	1.34 ± 0.41	1.40 ± 0.48	0.56	0.40	0.71
n	2.33 ± 0.15	2.34 ± 0.11	2.26 ± 0.14	0.97	0.75	0.69

HC = healthy codominant; HD = healthy dominant; HN = healthy nondominant.
Morphological parameters in healthy controls, evaluated based on flow and size as the dominant A1 (A1 is 20% larger than the other A1 segment), nondominant (A1 is 20% smaller than the other A1 segment), and codominant A1 (the two A1 segments have comparable sizes [within 20% difference]). Boldface type indicates statistical significance.

eurysms have the lowest female predominance of all aneurysms.[5]

Cerebral bifurcations are preferred sites for intracranial aneurysm formation, making their morphology a focus of aneurysm research. Multiple studies have evaluated healthy and aneurysmal bifurcation morphology of locations with a high risk of occurrence such as the MCA,[8,11,13,15,19–21] anterior communicating artery,[22–26] and basilar artery.[14,21,27] ICAB aneurysms occur at a relative low incidence, so the evaluation of ICAB morphology is limited to a small number of patients,[9,28] aggregate studies evaluating multiple locations,[8] or studies with no healthy controls.[10] Here, we compare ICAB morphology between aneurysmal, contralateral, and healthy bifurcations, including matched-pair bilateral analysis, effect of anterior cerebral artery dominance, and analysis of the VOP.

Our results showed that Φ_{ICAB}, as well as the angles formed between the ICA and daughter vessels (Φ_{MCA} and Φ_{ACA}), were significantly wider in aneurysmal versus control ICABs. In particular, Φ_{MCA} was a strong discriminator of aneurysmal status (AUC = 0.83). In multivariate analysis, Φ_{MCA} (threshold value 51.7°) and Φ_{ICAB} (threshold value 152.4°) combined resulted in an AUC of 0.85 (78% sensitivity, 78% specificity) in discriminating between aneurysmal and nonaneurysmal ICABs. Based on angle threshold analysis, 5 (12.5%) aneurysmal ICABs would be misclassified as healthy bifurcations. The misclassification occurred predominantly in smaller aneurysms as 4 of the 5 aneurysms were smaller than 3 mm. There were no significant differences regarding vessel caliber and radius ratios between aneurysmal and control groups.

Aneurysms occurred predominantly at the apex and off the A1 segment, with only 5% originating off the M1 segment. In addition, aneurysms occurred predominantly

TABLE 3. Matched-pair statistical analysis of ICAB parameters

Feature	Aneurysmal vs Contralat, n = 28		HD vs HN, n = 33	
	Mean ± SD	p Value	Mean SD	p Value
Φ_{MCA}, °	57.59 ± 12.22 vs 41.79 ± 10.98	**<0.001**	46.54 ± 8.69 vs 40.25 ± 8.90	**0.002**
Φ_{ACA}, °	104.05 ± 15.71 vs 93.32 ± 12.00	**0.02**	94 ± 9.28 vs 104.32 ± 10.98	**<0.001**
Φ_{ICAB}, °	161.65 ± 16.16 vs 135.12 ± 12.69	**<0.001**	141.16 ± 9.35 vs 144.57 ± 12.21	0.12
d_{MCA}, mm	2.47 ± 0.44 vs 2.37 ± 0.51	0.24	2.61 ± 0.27 vs 2.60 ± 0.31, p = 0.71	0.71
d_{ACA}, mm	1.93 ± 0.42 vs 1.87 ± 0.49	0.52	2.27 ± 0.30 vs 1.64 ± 0.37	**<0.001**
d_{ICA}, mm	3.16 ± 0.33 vs 3.10 ± 0.54	0.58	3.35 ± 0.42 vs 3.11 ± 0.41	**0.001**
d_{ICA}/d_{MCA}	1.29 ± 0.22 vs 1.36 ± 0.19	0.43	1.29 ± 0.13 vs 1.20 ± 0.13	**0.003**
d_{ICA}/d_{ACA}	1.71 ± 0.34 vs 1.79 ± 0.69	0.61	1.49 ± 0.20 vs 1.98 ± 0.46	**<0.001**
RR	1.50 ± 0.60 vs 1.61 ± 0.65	0.25	1.29 ± 0.35 vs 1.40 ± 0.48	0.15
n	2.26 ± 0.91 vs 1.96 ± 0.17	0.13	2.33 ± 0.15 vs 2.26 ± 0.14	0.59

ICAB parameters between the aneurysmal ICA side and corresponding nonaneurysmal contralateral ICA, and between healthy controls in which the contralateral A1 segments are labeled as dominant and nondominant based on vessel diameter. Resulting p values may differ slightly from univariate analyses due to the use of matched-pair methodology. Boldface type indicates statistical significance.

Not for reprint

Low-resolution PDF

on dominant and codominant ICABs (labeled based on A1 dominance) and only 10% occurred on ICABs with nondominant A1 segments. No correlation was found between aneurysm size and Φ_{MCA}, Φ_{ACA}, and Φ_{ICAB}. However, similar to reports on MCA[13] and basilar bifurcations,[14] the aneurysm neck was positively correlated with bifurcation angles, in our case Φ_{MCA} and Φ_{ICAB} but not Φ_{ACA}. It should be noted that, despite higher Φ_{MCA} being correlated with a larger neck, only 5% of all aneurysms originated off the MCA branch. Moreover, there was no correlation between age and Φ_{MCA}, Φ_{ACA}, and Φ_{ICAB} regardless of aneurysm presence. This contrasts with reports on MCA[13] and basilar artery bifurcations,[14] which found positive angle correlations with age. These differences might explain why ICAB aneurysms occur at younger ages and are predominant in pediatric cases. Younger age at occurrence and lack of angle correlation with age could also support the hypothesis that wider ICAB angles precede aneurysm formation.

In contrast to tree-like structures describing most cerebral bifurcations, ICABs are part of the circle of Willis, where the confluence of hemodynamic patterns differs from typical vascular branching. The hemodynamics of the circle of Willis are shaped by variations in the size of the communicating arteries and the segments of the anterior and posterior cerebral arteries. In this context of interconnectedness, we evaluated healthy ICABs bilaterally, considering the dominance status of the A1 segments. Although smaller compared with aneurysmal ICABs, healthy dominant ICABs exhibited similar angle characteristics, with a wider dominant Φ_{MCA} and smaller dominant Φ_{ACA}. This resulted in similar total bifurcation angles regardless of the dominance, which were significantly smaller compared with aneurysmal bifurcations.

Regarding VOP, Rossitti and Löfgren[9] proposed a theoretical optimum value of 3 for bifurcation *n* and an optimal value of 1 for RR. Ingebrigtsen et al.[8] showed that, whereas MCA bifurcations closely approximate these values, ICA and basilar bifurcations do not. Additional work by Baharoglu et al.[11] further showed that healthy MCA bifurcations follow VOP and have optimal RR and *n* values; however, aneurysmal bifurcations do not. Our results show that both aneurysmal and healthy ICABs have a RR larger than 1 and *n* smaller than 3. These values are consistent with previously reported VOP measurements of ICAB.[8,29] Ingebrigtsen et al.[8] concluded that because of their location within the circle of Willis, ICABs do not follow VOP. However, work by Zamir[30] and Chnafa et al.[29] suggested that optimal *n* values for larger vessels such as the ICA may be closer to 2 rather than 3. Regardless of what optimality means for ICABs, our results show that RR and *n* values are not significantly different based on ICAB aneurysm presence, in contrast to reports on MCA bifurcations.[11]

Overall, aneurysmal and healthy ICABs have distinct morphology stemming from the ICAB position within the circle of Willis. Despite common characteristics, aneurysmal and healthy ICABs show important differences in their angular morphology, which provides new insights into how the bifurcation morphology might be related to a higher risk of aneurysm presence. Our study is retrospective in nature, and its clinical relevance would need to be confirmed in a prospective fashion, but using the conclusion of this study, including the identification of angle thresholds which discriminate between healthy and aneurysmal bifurcations, could potentially be used to monitor and screen patients who are asymptomatic, have a family history of aneurysms, or have been identified of being at risk for developing multiple aneurysms. Our research regarding morphological predisposition to aneurysm development complements existing findings on how morphology affects clinical outcomes. Prior research suggested that "T-shaped" bifurcation morphology, such as ICAB, are associated with better clinical outcomes compared with "non–T-shaped" morphology even in the presence of comparable adverse factors.[31] Our study contributes to this framework by suggesting that while wider ICAB configurations might be more prone to aneurysm development, they may also confer a more favorable prognosis once rupture occurs. This highlights the clinical utility of integrating morphological assessments into both risk prediction and treatment planning. Additionally, prior research on basilar artery bifurcations[32,33] has shown that Y-configuration stent-assisted coiling has the potential to alter the native vascular angulation, resulting in vascular remodeling that could impact the long-term risk of recurrence. Whether similar interventions at the ICAB can induce beneficial remodeling and how that might relate to both aneurysm stability and outcome remains an open question. Hemodynamic studies and prospective analysis are required to determine if vascular remodeling also occurs at the ICAB following specific interventions, and what its implications are for clinical outcomes.

Study Limitations

As with similar retrospective research, the association between bifurcation morphology and aneurysm presence suggests a correlation but does not imply causation, a limitation shared with all similar research. Given the retrospective nature of our study, we cannot conclude that wider bifurcation angles preceded aneurysm formation, and aneurysm formation might have altered bifurcation morphology itself. A prospective analysis of a small set of MCA bifurcations[19] seems to suggest that wide branching angles precede aneurysm formation whereas analysis of healthy basilar artery bifurcations showed that bifurcation angles were positively correlated with age.[14] However, to the best of our knowledge, no conclusive data have yet been presented to address this issue. It is possible that aneurysm formation is an epiphenomenon associated with wider bifurcations, rather than a direct result of higher-risk morphology. It should be noted that many small aneurysms in this study occurred at wide bifurcations. Moreover, although the angle formed between the ICA and MCA branches was strongly correlated with aneurysm presence, only 5% of the aneurysms originated off the MCA, an argument against angle alteration after aneurysm origination.

Furthermore, the conclusions of this study are based on the morphological analysis of the ICAB. Hemodynamic evaluation and clinical risk factors—such as smoking, hypertension, and family history of intracranial aneurysms—were not considered. Future studies should integrate mor-

Not for reprint

Low-resolution PDF

phological assessments with these additional factors for a more complete understanding of aneurysm development and associated risks. Therefore, the conclusions of this study will require validation by further research.

Conclusions

Aneurysmal ICABs are associated with larger bifurcation angles, more so on the MCA side. The angles of Φ_{MCA} (AUC = 0.83) and Φ_{ICAB} (AUC = 0.79) were the best discriminators of aneurysm status in univariate, multivariate (AUC = 0.85), and matched-pair bilateral analyses. Angle thresholds of 51.7° for Φ_{MCA} and 152.4° for Φ_{ICAB} were determined by ROC analysis. Aneurysms originated predominantly off the apex (65%) and ACA branch (30%). Most aneurysms occurred on ICAB with dominant (31%) and codominant (58%) A1 segments. In healthy patients, Φ_{MCA} was significantly greater and Φ_{ACA} was significantly smaller on the dominant side, with no Φ_{ICAB} difference. ICABs had similar RR and *n* values regardless of aneurysm presence and dominance status. These findings underline the importance of ICAB morphology for the likelihood of aneurysm presence, an association that can inform clinical decisions and may serve in predictive analytics. The conclusions of this study will require validation by further research.

References

1. Sforza DM, Putman CM, Cebral JR. Hemodynamics of cerebral aneurysms. *Annu Rev Fluid Mech*. 2009;41(1):91-107.
2. Morales-Valero SF, Brinjikji W, Murad MH, Wald JT, Lanzino G. Endovascular treatment of internal carotid artery bifurcation aneurysms: a single-center experience and a systematic review and meta-analysis. *AJNR Am J Neuroradiol*. 2014;35(10):1948-1953.
3. van Rooij WJ, Sluzewski M, Beute GN. Internal carotid bifurcation aneurysms: frequency, angiographic anatomy and results of coiling in 50 aneurysms. *Neuroradiology*. 2008; 50(7):583-587.
4. Lehecka M, Dashti R, Romani R, et al. Microneurosurgical management of internal carotid artery bifurcation aneurysms. *Surg Neurol*. 2009;71(6):649-667.
5. Gupta SK, Khosla VK, Chhabra R, et al. Internal carotid artery bifurcation aneurysms: surgical experience. *Neurol Med Chir (Tokyo)*. 2007;47(4):153-158.
6. Huang J, McGirt MJ, Gailloud P, Tamargo RJ. Intracranial aneurysms in the pediatric population: case series and literature review. *Surg Neurol*. 2005;63(5):424-432.
7. van Rooij WJ, Sprengers ME, de Gast AN, Peluso JPP, Sluzewski M. 3D rotational angiography: the new gold standard in the detection of additional intracranial aneurysms. *AJNR Am J Neuroradiol*. 2008;29(5):976-979.
8. Ingebrigtsen T, Morgan MK, Faulder K, Ingebrigtsen L, Sparr T, Schirmer H. Bifurcation geometry and the presence of cerebral artery aneurysms. *J Neurosurg*. 2004;101(1):108-113.
9. Rossitti S, Löfgren J. Vascular dimensions of the cerebral arteries follow the principle of minimum work. *Stroke*. 1993; 24(3):371-377.
10. Akdağ R, Soylu U, Uçkun ÖM, Polat Ö, Gürpınar İ, Dağlıoğlu E. Aneurysm formation at the internal carotid artery bifurcation is related to the vascular geometry of the bifurcation. *Brain Sci*. 2024;14(12):1247.
11. Baharoglu MI, Lauric A, Wu C, Hippelheuser J, Malek AM. Deviation from optimal vascular caliber control at middle cerebral artery bifurcations harboring aneurysms. *J Biomech*. 2014;47(13):3318-3324.
12. Rossitti S, Löfgren J. Optimality principles and flow orderliness at the branching points of cerebral arteries. *Stroke*. 1993; 24(7):1029-1032.
13. Baharoglu MI, Lauric A, Safain MG, Hippelheuser J, Wu C, Malek AM. Widening and high inclination of the middle cerebral artery bifurcation are associated with presence of aneurysms. *Stroke*. 2014;45(9):2649-2655.
14. Tütüncü F, Schimansky S, Baharoglu MI, et al. Widening of the basilar bifurcation angle is associated with presence of intracranial aneurysm, age, and female gender. *J Neurosurg*. 2014;121(6):1401-1410.
15. Sadatomo T, Yuki K, Migita K, Imada Y, Kuwabara M, Kurisu K. Differences between middle cerebral artery bifurcations with normal anatomy and those with aneurysms. *Neurosurg Rev*. 2013;36(3):437-445.
16. Bescos JO, Slob MJ, Slump CH, Sluzewski M, van Rooij WJ. Volume measurement of intracranial aneurysms from 3D rotational angiography: improvement of accuracy by gradient edge detection. *AJNR Am J Neuroradiol*. 2005;26(10):2569-2572.
17. Antonov A, Kono K, Greim-Kuczewski K, Hippelheuser JE, Lauric A, Malek AM. Proximal stenosis is associated with rupture status in middle cerebral artery aneurysms. *World Neurosurg*. 2018;109:e835-e844.
18. Juvela S, Porras M, Poussa K. Natural history of unruptured intracranial aneurysms: probability and risk factors for aneurysm rupture. *J Neurosurg*. 2000;93(3):379-387.
19. Bor AS, Velthuis BK, Majoie CB, Rinkel GJ. Configuration of intracranial arteries and development of aneurysms: a follow-up study. *Neurology*. 2008;70(9):700-705.
20. Lauric A, Greim-Kuczewski K, Antonov A, et al. Proximal parent vessel tapering is associated with aneurysm at the middle cerebral artery bifurcation. *Neurosurgery*. 2019;84(5): 1082-1089.
21. Ćmiel-Smorzyk K, Kawlewska E, Wolański W, Hebda A, Ładziński P, Kaspera W. Morphometry of cerebral arterial bifurcations harbouring aneurysms: a case-control study. *BMC Neurol*. 2022;22(1):49.
22. Sadatomo T, Yuki K, Migita K, Taniguchi E, Kodama Y, Kurisu K. The characteristics of the anterior communicating artery aneurysm complex by three-dimensional digital subtraction angiography. *Neurosurg Rev*. 2006;29(3):201-207.
23. Lauric A, Silveira L, Lesha E, Breton JM, Malek AM. Aneurysm presence at the anterior communicating artery bifurcation is associated with caliber tapering of the A1 segment. *J Neurosurg*. 2022;136(6):1694-1704.
24. Cai W, Hu C, Gong J, Lan Q. Anterior communicating artery aneurysm morphology and the risk of rupture. *World Neurosurg*. 2018;109:119-126.
25. Flores BC, Scott WW, Eddleman CS, Batjer HH, Rickert KL. The A1-A2 diameter ratio may influence formation and rupture potential of anterior communicating artery aneurysms. *Neurosurgery*. 2013;73(5):845-853.
26. Krzyzewski RM, Tomaszewska IM, Lorenc N, et al. Variations of the anterior communicating artery complex and occurrence of anterior communicating artery aneurysm: A2 segment consideration. *Folia Med Cracov*. 2014;54(1):13-20.
27. Ambekar S, Madhugiri V, Bollam P, Nanda A. Morphological differences between ruptured and unruptured basilar bifurcation aneurysms. *J Neurol Surg B Skull Base*. 2013; 74(2):91-96.
28. Sakamoto S, Ohba S, Shibukawa M, et al. Characteristics of aneurysms of the internal carotid artery bifurcation. *Acta Neurochir (Wien)*. 2006;148(2):139-143.
29. Chnafa C, Bouillot P, Brina O, et al. Vessel calibre and flow splitting relationships at the internal carotid artery terminal bifurcation. *Physiol Meas*. 2017;38(11):2044-2057.

Not for reprint

Low-resolution PDF

30. Zamir M. Optimality principles in arterial branching. *J Theor Biol*. 1976;62(1):227-251.
31. Brawanski N, Bruder M, Won SY, et al. Comparison of carotid and basilar bifurcation aneurysms versus non-T-angled bifurcations: the geometry is associated with the outcome. *Neurosurg Rev*. 2019;42(4):853-858.
32. Gao B, Baharoglu MI, Cohen AD, Malek AM. Stent-assisted coiling of intracranial bifurcation aneurysms leads to immediate and delayed intracranial vascular angle remodeling. *AJNR Am J Neuroradiol*. 2012;33(4):649-654.
33. Gao B, Baharoglu MI, Cohen AD, Malek AM. Y-stent coiling of basilar bifurcation aneurysms induces a dynamic angular vascular remodeling with alteration of the apical wall shear stress pattern. *Neurosurgery*. 2013;72(4):617-629.

Disclosures

Dr. Malek reported consulting for CereVasc Inc. and Stryker Inc. outside the submitted work.

Author Contributions

Conception and design: Malek. Acquisition of data: Lauric. Analysis and interpretation of data: both authors. Drafting the article: Lauric. Critically revising the article: Malek. Approved the final version of the manuscript on behalf of both authors: Malek. Statistical analysis: Lauric. Study supervision: Malek.

Supplemental Information

Online-Only Content

Supplemental material is available with the online version of the article.

Supplemental Table 1. https://thejns.org/doi/suppl/10.3171/2025.8.JNS25106.

Correspondence

Adel M. Malek: Tufts Medical Center, Boston, MA. amalek@tuftsmedicalcenter.org.

Not for reprint